

- molecular structure and multimer formation of adiponectin. *J Biol Chem* 2003;278:40352–63.
7. Hada Y, Yamauchi T, Waki H, Tsuchida A, Hara K, Yago H, et al. Selective purification and characterization of adiponectin multimer species from human plasma. *Biochem Biophys Res Commun* 2007;356:487–93.
 8. Pajvani UB, Hawkins M, Combs TP, Rajala MW, Doebber T, Berger JP, et al. Complex distribution, not absolute amount of adiponectin, correlates with thiazolidinedione-mediated improvement in insulin sensitivity. *J Biol Chem* 2004;279:12152–62.
 9. Hara K, Horikoshi M, Yamauchi T, Yago H, Miyazaki O, Ebinuma H, et al. Measurement of the high-molecular-weight form of adiponectin in plasma is useful for the prediction of insulin resistance and metabolic syndrome. *Diabetes Care* 2006;29:1357–62.
 10. Ebinuma H, Miyazaki O, Yago H, Hara K, Yamauchi T, Kadowaki T. A novel ELISA system for selective measurement of human adiponectin multimers by using proteases. *Clin Chim Acta* 2006;372:47–53.
 11. Yoshida H. [Histological view of ethics in medicine and handling of residual samples in clinical laboratories.] *Rinsho Byori* 2004;52:231–5.
 12. Numata Y, Morita A, Kosugi Y, Shibata K, Takeuchi N, Uchida K. New sandwich ELISA for human urinary N-acetyl-beta-D-glucosaminidase isoenzyme B as a useful clinical test. *Clin Chem* 1997;43:569–74.
 13. Wang Y, Xu A, Knight C, Xu LY, Cooper GJ. Hydroxylation and glycosylation of the four conserved lysine residues in the collagenous domain of adiponectin: potential role in the modulation of its insulin-sensitizing activity. *J Biol Chem* 2002;277:19521–9.
 14. Kusminski CM, McTernan PG, Schraw T, Kos K, O'Hare JP, Ahima R, et al. Adiponectin complexes in human cerebrospinal fluid: distinct complex distribution from serum. *Diabetologia* 2007;50:634–42.

Previously published online at DOI: 10.1373/clinchem.2007.085654

Expanded Instrument Comparison of Amplicon DNA Melting Analysis for Mutation Scanning and Genotyping, Mark G. Herrmann,^{1*} Jacob D. Durtschi,¹ Carl T. Wittwer,^{1,2} and Karl V. Voelkerding^{1,2} (¹Institute for Clinical and Experimental Pathology, ARUP, Salt Lake City, UT; ²Department of Pathology, University of Utah School of Medicine, Salt Lake City, UT; * address correspondence to this author at: ARUP Laboratories, 500 Chipeta Way, Salt Lake City, UT 84108; fax 801-584-5114, e-mail mark.herrmann@aruplab.com)

Background: Additional instruments have become available since instruments for DNA melting analysis of PCR products for genotyping and mutation scanning were compared. We assessed the performance of these new instruments for genotyping and scanning for mutations.

Methods: A 110-bp fragment of the β -globin gene including the sickle cell anemia locus (*HBB* c. 20A>T) was amplified by PCR in the presence of LCGreen Plus or SYBR Green I. Amplicons of 4 different genotypes [wild-type, homozygous, and heterozygous *HBB* c. 20A>T and double-heterozygote *HBB* c. (9C>T; 20A>T)] were melted on 7 different instruments [Applied Biosystems 7300, Corbett Life Sciences Rotor-Gene 6500HRM, Eppendorf Mastercycler RealPlex4S, Idaho Technology LightScanner (384 well), Roche LightCycler 480 (96 and 384 well) and Stratagene Mx3005p] at a rate of 0.61 °C/s or when this was not possible, at 0.50 °C steps. We evaluated the ability of each instrument to genotype by melting temperature (T_m) and to scan for heterozygotes by curve shape.

Results: The ability of most instruments to accurately genotype single-base changes by amplicon melting was limited by spatial temperature variation across the plate (SD of T_m = 0.020 to 0.264 °C). Other variables such as data density, signal-to-noise ratio, and melting rate also affected heterozygote scanning.

Conclusions: Different instruments vary widely in their ability to genotype homozygous variants and scan for heterozygotes by whole amplicon melting analysis. Instruments specifically designed for high-resolution melting, however, displayed the least variation, suggesting better genotyping accuracy and scanning sensitivity and specificity.

© 2007 American Association for Clinical Chemistry

Melting curve analysis has grown in sophistication from genotyping single-base variants with fluorescence resonance energy transfer probes (1) to inferring and differentiating sequence homologies through high-resolution amplicon melting with DNA binding dyes (2–4). These advanced techniques are already being adapted to existing real-time PCR instruments. In our prior studies (5, 6), we evaluated the melting capabilities of 9 melting instruments found in our laboratory. These instruments varied in ability to detect homozygous mutants as well as to identify single- and double-heterozygous samples. The ability to differentiate complex melting species depends on the quality of the melting curve generated. Since our initial reports, 7 additional instruments have become available for genotyping and heterozygote scanning. Understanding the melting capabilities of these instruments should guide the appropriate use of different techniques.

As previously described (5, 6), a 110-bp fragment of the β -globin gene including the sickle cell anemia locus (*HBB* c. 20A>T) was amplified by PCR in the presence of a DNA binding dye. A single patient sample of each genotype [wild-type, homozygous, and heterozygous *HBB* c. 20A>T and double-heterozygote *HBB* c. (9C>T; 20A>T)] were amplified, pooled by genotype, and reallocated for instrument evaluation. Melting curves were obtained with the Applied Biosystems 7300, Corbett Life Science Rotor-Gene[™] 6500HRM, Eppendorf Mastercycler[®] RealPlex4S, Idaho Technology LightScanner[®] (384 well), Roche LightCycler[®] 480 (96- and 384-well models), and Stratagene Mx3005p[™]. Melting curves were obtained at 0.1 °C/s if possible. For instruments able to perform only step monitoring, the melting cycle was monitored at 10 acquisitions/°C with a 10-s hold. A single 96/384-well plate or 72-sample rotor containing homogenous wild-type amplicon and LCGreen[®] Plus (Idaho Technology) were used to determine temperature homogeneity [expressed as the melting temperature (T_m) SD], melting curve superimposability (expressed as the temperature-shifted T_m SD), signal-to-noise ratio, data density, and, for the heat block instruments, dynamic thermal profiles. Because of spectral incompatibilities with LCGreen Plus,

SYBR Green I (Invitrogen) was used with the Stratagene's Mx3005p.

Heterozygote scanning was also evaluated by melting each of the 4 genotypes in triplicate. For heat block instruments, the amplicons were placed in identical positions randomly dispersed across the plate, with an equal volume of water filling the intervening spaces. The resulting melting curves were temperature-shifted for resolving single- and double-heterozygous samples.

The normalized melting curves are shown in Fig. 1A. The apparent temperature variation within a genotype was highly dependent on the instrument used. After temperature shifting, the T_m variation within a genotype was usually decreased (Fig. 1B), particularly in the case of the 7300 and LC480 instruments, for which temperature shifting enabled heterozygote differentiation. The displacement of the double heterozygote was so great that it was distinguishable in all cases, but accurate detection of the single heterozygote was not achieved with all instruments.

Table 1 shows instrument variables and measured T_m SDs compiled from this and prior studies (5, 6). The T_m SDs directly affect the ability to separate different homozygous melting curves. The main contributing variable appears to be temperature homogeneity. As seen previously, air-based instruments and instruments with individual sample temperature control have lower T_m SDs (0.018–0.065) than their heat-block counterparts (0.092–0.274). Block systems with thermal electric heaters had lower T_m SDs (0.092–0.102) than Peltier-based systems (0.117–0.274). The dynamic melting profile for the 96-well and 384-well heat blocks are shown in Fig. 1C. Thermal edge effects and the Peltier configuration can be inferred from the thermal maps of the heat block instruments.

Genotyping single-base variants with fluorescent probes usually results in T_m differences for the matched and mismatched species of 4–10 °C. All the instruments studied are capable of genotyping at this level of resolution. When genotyping is performed by amplicon melting, however, T_m differences are much smaller. The mean T_m difference of homozygotes of class 1 and class 2 single-nucleotide polymorphisms (SNPs) was 1 °C, and almost all have a T_m difference >0.5 °C (7). In 8 of the instruments, estimated error rates were <1% at this degree of resolution (SD <0.109) (5). When the melting difference was decreased to >0.25 °C, as in typical class 3 and class 4 SNPs, only 5 of the instruments evaluated had an estimated error rate of <1% (SD >0.054).

Different homozygotes each produce only a single homoduplex species. Therefore, genotyping by T_m (determined as the temperature at 50% of the normalized fluorescence) is straightforward and has an accuracy directly correlated to temperature homogeneity. The T_m variation of block-based systems is greater than that for air-based or individual sample systems. This variation is attributable to difficulties in uniformly heating large metal blocks and assigning a single temperature to repre-

sent the entire block. The thermal control of multiple samples is improved with air-based systems, for which rapid mixing forces temperature homogeneity. Alternatively, single-sample systems also fared well, because spatial temperature homogeneity is not a concern, allowing better temperature control and measurement.

Detection of heterozygous samples by amplicon melting is more complex than homozygote differentiation. Heterozygotes differ primarily in melting curve shape rather than absolute T_m . These differences are often visualized after temperature shifting to superimpose the curves, allowing easy visualization and grouping by melting curve shape. For any heterozygous sample, the resulting melting curve is a combination of 2 homoduplexes and 2 heteroduplexes that form as the samples are cooled. Mismatched duplexes melt at lower temperatures than homoduplexes. For example, PCR of the single heterozygote (*HBB* c. 20A>T) produces duplexes with predicted T_m s (7) of 85.89 and 85.80 °C for the homoduplexes and 85.11 and 85.10 °C for the heteroduplexes. The resulting melting curves on most instruments show 2 melting regions, a lower temperature region of heteroduplex melting and a higher region of homoduplex melting. The double-heterozygous sample [*HBB* c. (9C>T; 20A>T)] again is composed of 2 heteroduplexes with predicted T_m s of 84.41 and 84.51 °C and 2 homoduplexes with predicted T_m s of 85.36 and 85.89 °C. In this case, the 2 homoduplex species are separated by 0.53 °C and can be distinguished on some instruments. The ability to resolve subtleties in the melting curve requires more than a single T_m for proper identification. The melting curve shape of heterozygotes depends on the number of discrete melting populations, the sharpness of each transition, and the different stabilities of each species.

About half of the instruments surveyed performed heterozygote scanning well. Multiple variables affect the quality of DNA melting curves, including data density, signal-to-noise ratio, and melting rate. For example, increasing the data density beyond 10 points/°C allows for more melting information to be displayed and potentially the resolution of more duplex species. In addition, the 3 melting domains of the double heterozygotes were easier to resolve in melting curves with higher signal-to-noise ratios and good superimposability (low temperature-shifted T_m SD). Improved resolution also becomes important in recognizing unknown variants that occur within the amplicon studied (8). Prior reports suggest that better heteroduplex detection is obtained at faster melting rates and higher signal-to-noise ratios (9). Although a general correlation with these factors was observed, the significance of each factor and their interactions will require further study.

Limitations of the current study include the assumption that each instrument and its performance are typical. For a few instruments additional runs were performed and did not significantly differ from those reported (data

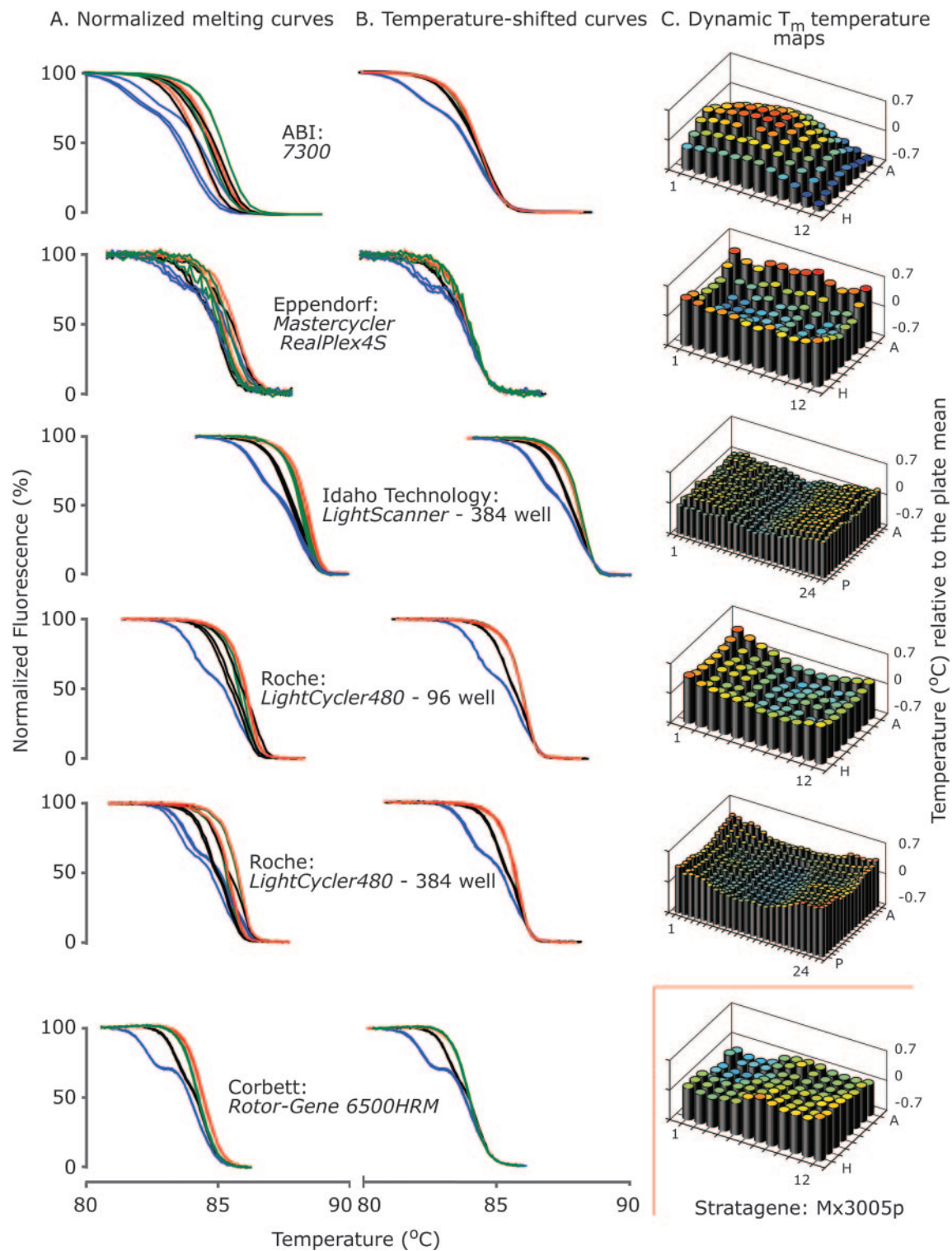


Fig. 1. Normalized and temperature-shifted melting curves of a 110-bp β -globin amplicon and the associated thermal profiles of heat block instruments.

Each genotype was melted and displayed in triplicate on the different instruments. Melting curves for the homozygous wild type are shown in *green*, homozygous mutant (c. 20A>T) in *red*, the single-heterozygous mutant (c. 20A>T) in *black*, and the double-heterozygote mutant [c. (9C>T; 20A>T)] in *blue*. (A), normalized melting curves of each instrument studied. (B), temperature-shifted melting curves used for heterozygote scanning. (C), the dynamic melting profile of all plate instruments referenced to the mean T_m of the wild-type amplicon. LCGreen Plus was used as the dye, except on the Stratagene Mx3005p, which required use of SYBR Green I.

Table 1. Instrument and sample characteristics.

Instrument	Sample and thermal format	Acquisition mode	Data points/°C	Melting rates, ^a °C/s	Melting time, min	S/N ^b	T _m SD, ^c °C	T _m SD _{ts} , ^{c,d} °C	n	T _m range, ^e °C
LCGreen Plus-compatible										
ABI: 7000	96-well plate, Peltier	Cont.	3.1	0.022	27.0	560	0.117	0.065	96	0.66
ABI: 7300	96-well plate, Peltier	Cont.	2.7	0.036	16.0	<i>f</i>	0.263	<i>f</i>	96	1.02
Bio-Rad: iCycler	96-well plate, Peltier	Step	10	0.009	65.0	410	0.173	0.064	96	1.10
Cepheid: SmartCycler	1 square tube, thermal electric/air	Cont.	10	0.100	5.8	310	0.065	0.051	32	0.22
Corbett: Rotor-Gene 3000	72 tubes, circulating air	Step	10	0.008	73.0	180	0.045	0.051	72	0.19
Corbett: Rotor-Gene 6500HRM	72 tubes, circulating air	Step	10	0.006	97.0	300	0.020	0.028	72	0.09
Eppendorf: Mastercycler RealPlex4S	96-well plate, Peltier	Cont.	10	0.012	49.0	90	0.226	0.042	96	0.87
Idaho Technology: HR-1	1 glass capillary, thermal electric	Cont.	200	0.100	5.8	3500	0.018	0.012	32	0.06
Idaho Technology: LightScanner (384)	384-well plate, thermal electric	Cont.	12	0.105	6.0	520	0.096	0.024	384	0.45
Idaho Technology: LightScanner (96)	96-well plate, thermal electric	Cont.	14	0.100	5.8	1800	0.092	0.013	96	0.35
Roche: LightCycler 1.2	32 glass capillaries, circulating air	Cont.	5.2	0.100	5.9	260	0.045	<i>f</i>	32	0.19
Roche: LightCycler 2.0	32 glass capillaries, circulating air	Cont.	4.1	0.100	6.5	490	0.047	<i>f</i>	32	0.18
Roche: LightCycler 480 (384)	384-well plate, Peltier	Cont.	10	0.090	7.3	460	0.160	0.017	384	0.71
Roche: LightCycler 480 (96)	96-well plate, Peltier	Cont.	10	0.110	6.3	670	0.144	0.014	96	0.67
SYBR Green I-compatible										
ABI: 7900HT	96-well plate	Cont.	4.2	0.014	42.0	180	0.274	<i>f</i>	96	1.24
Stratagene: Mx3005p	96-well plate	Cont.	1.9	0.030	19.0	60	0.139	0.090	96	0.61
		Step	10	0.009	65.0	60	0.159	0.060	96	0.50

^a Observed melting rates (programmed at 0.1 °C/s when possible).

^b S/N, signal-to-noise ratio as determined in Ref. 1.

^c SD of the T_m within a genotype for normalized melting curves (relevant to genotyping and instrument temperature homogeneity).

^d SD of the T_m within a genotype after temperature-shifting (relevant to heterozygote scanning and melting curve superimposability).

^e Temperature range of T_m based on n values.

^f Calculation not possible.

not shown). Another concern is that the number of samples studied was influenced by the sample capacity of each instrument (96 or 384 for plates and 72 or 32 for rotors). These within-run variations were compared to 32 interrun variances on single sample instruments.

Melting curve analysis with saturating DNA dyes is a simple method for genotyping and scanning (7). Homozygous samples can often be genotyped by an absolute change in T_m (10), while heterozygous samples can be identified through changes in the shape of the melting curve (11,12). Recently, internal temperature controls have been used to correct for T_m variation seen in low-resolution instruments (13–15). These controls provide a reference to correctly genotype homozygous alleles regardless of the temperature homogeneity of the system. The detection of subtle sequence changes for variant scanning will continue to rely on the resolution of melting instruments.

Grant/funding support: Applied Biosystems, Corbett Life Science, Eppendorf, Idaho Technology, and Stratagene provided access to demonstration instruments, which were temporarily placed in the ARUP laboratory for this evaluation. The project was otherwise funded solely by ARUP Laboratories.

Financial disclosures: Aspects of melting analyses are covered by issued and pending patents owned by the University of Utah and licensed to Idaho Technology. C.T.W. holds equity interest in Idaho Technology.

Acknowledgments: We thank Applied Biosystems, Corbett Life Science, Eppendorf, Idaho Technology, and Stratagene for technical support during this evaluation and thank the reviewers and editors for valuable comments.

References

1. Lay MJ, Wittwer CT. Real-time fluorescence genotyping of factor V Leiden during rapid-cycle PCR. *Clin Chem* 1997;43:2262–7.
2. Krypuy M, Newnham GM, Thomas DM, Conron M, Dobrovic A. High resolution melting analysis for the rapid and sensitive detection of mutations in clinical samples: KRAS codon 12 and 13 mutations in non-small cell lung cancer. *BMC Cancer* 2006;6:295.
3. Reed GH, Wittwer CT. Sensitivity and specificity of single-nucleotide polymorphism scanning by high-resolution melting analysis. *Clin Chem* 2004;50:1748–54.
4. Zhou L, Vandersteen J, Wang L, Fuller T, Taylor M, Palais B, et al. High-resolution DNA melting curve analysis to establish HLA genotypic identity. *Tissue Antigens* 2004;64:156–64.
5. Herrmann MG, Durtschi JD, Bromley LK, Wittwer CT, Voelkerding KV. Amplicon DNA melting analysis for mutation scanning and genotyping: cross-platform comparison of instruments and dyes. *Clin Chem* 2006;52:494–503.
6. Herrmann MG, Durtschi JD, Bromley LK, Wittwer CT, Voelkerding KV. Instrument comparison for heterozygote scanning of single and double heterozygotes: a correction and extension of Herrmann et al. *Clin Chem* 2006;52:494–503. *Clin Chem* 2007;53:150–2.
7. Liew M, Pryor R, Palais R, Meadows C, Erali M, Lyon E, et al. Genotyping of single-nucleotide polymorphisms by high-resolution melting of small amplicons. *Clin Chem* 2004;50:1156–64.
8. Graham R, Liew M, Meadows C, Lyon E, Wittwer CT. Distinguishing different DNA heterozygotes by high-resolution melting. *Clin Chem* 2005;51:1295–8.
9. Gundry CN, Vandersteen JG, Reed GH, Pryor RJ, Chen J, Wittwer CT. Amplicon melting analysis with labeled primers: a closed-tube method for differentiating homozygotes and heterozygotes. *Clin Chem* 2003;49:396–406.
10. Palais RA, Liew MA, Wittwer CT. Quantitative heteroduplex analysis for single nucleotide polymorphism genotyping. *Anal Biochem* 2005;346:167–75.
11. Wittwer CT, Reed GH, Gundry CN, Vandersteen JG, Pryor RJ. High-resolution genotyping by amplicon melting analysis using LCGreen. *Clin Chem* 2003;49:853–60.
12. Zhou L, Wang L, Palais R, Pryor R, Wittwer CT. High-resolution DNA melting analysis for simultaneous mutation scanning and genotyping in solution. *Clin Chem* 2005;51:1770–7.
13. Liew M, Seipp M, Durtschi J, Margraf RL, Dames S, Erali M, et al. Closed-tube SNP genotyping without labeled probes/a comparison between unlabeled probe and amplicon melting. *Am J Clin Pathol* 2007;127:1–8.
14. Nellaker C, Wallgren U, Karlsson H. Molecular beacon-based temperature control and automated analyses for improved resolution of melting temperature analysis using SYBR I Green chemistry. *Clin Chem* 2007;53:98–103.
15. Seipp M, Durtschi J, Liew M, Williams J, Damjanovich K, Pont-Kingdon G, et al. Unlabeled oligonucleotides as internal temperature controls for genotyping by amplicon melting. *J Mol Diagn* 2007;9:284–9.

DOI: 10.1373/clinchem.2007.088120
